International Journal of Scientific Research in Chemistry (IJSRCH)
© 2019 IJSRCH | Volume 4 | Issue 3 | ISSN : 2456-8457

A Review of Two-Dimensional Materials in Electrocatalysis and their Potential Applications

Jamilu Ya'u Muhammad*[1], Mika'il Abdulkarim Alhaji[2], Mohammed Abdullahi Gele[3], Ibrahim Musa[4]

*[1]Department of Mechanical Engineering, Bayero University, Kano, Nigeria

[2]Department of Physics, Federal University, Wukari, Nigeria

[3]Sokoto Energy Research Centre, Services Unit, Sokoto, Nigeria

[4]Department of Agricultural and Bio-Environmental Engineering, College of Agriculture, Zuru, Nigeria

ABSTRACT

Two-dimensional materials are crystalline materials consist of a single layer of atoms and sometimes referred to as single layer materials. Electrocatalytic energy conversion using renewable power sources is one of the most promising ways for energy storage and energy utilization in the new century. Over the past years, a great number of two-dimensional (2D) materials have been explored for various electrocatalytic reactions, such as the hydrogen evolution reaction, Carbon (IV) oxide (CO_2) reduction reaction and Oxygen (O_2) reduction reaction. This research provides an overview on the synthesis techniques of materials including bottom up approaches such as chemical vapor deposition (CVD) and physical vapor deposition (PVD) and top-down approaches like mechanical exfoliation, chemical exfoliation. Then, the characterization techniques of the two-dimensional (2D) materials such as Raman spectroscopy, X-ray diffraction, temperature-dependent resistivity and magnetic susceptibility and scanning tunneling microscopy (STM) are reviewed. Finally, potential applications of two-dimensional (2D) materials and conclusion, challenges and future work are discussed.

Keywords : Two-dimensional materials, Raman spectroscopy, Chemical Vapor Deposition (CVD), Mechanical Exfoliation

I. INTRODUCTION

Due to the rapid development of modern society, the enormous demand for energy has become one of the most important issues affecting human life since twentieth century [1]. Since the discovery of graphene in 2004 [2], there has been a quest for new two-dimensional (2D) materials. This new area of research with rapid growth from both theoretical and experimental fronts aimed at technological advancements.

Two dimensional materials, sometimes referred to as single layer materials, are crystalline materials consist of a single layer of atoms. These materials have found applicable in many areas such as photovoltaic [3, 4], semiconductors [5, 6], biomedical [7] and tissue engineering [8]. Two-dimensional materials have gained extensive attention since they exhibit novel and unique physical, chemical, mechanical, and electronic properties [9–14].

Two-dimensional materials are generally classified into two namely; two-dimensional allotropes of various elements (Graphene, Borophene and so on) and two-dimensional allotropes of various compound (Graphane, Molybdenite, Aerographite and many more) (made up of two or more covalently bonding

elements) [15]. The elemental two-dimensional materials generally carry the (-ene) suffix in their names while the compounds have (-ane or –ide) suffixes. Layered combinations of different two-dimensional materials are called Van der Waals heterostructures.

Recently, two-dimensional (2D) materials have been widely reported as promising non-noble material electrocatalysts due to their abundance, low cost, and highly efficient catalytic activity [16]. An electrocatalysis are catalysis that participates in electrochemical reactions. Catalyst materials madify and increase the rate of chemical reactions without being consumed in the process. Electrocatalysts are a specific form of catalysts that function at electrode surfaces or may be the electrodes surface itself. This can be heterogeneous (such as a platinum surface [17] and nanoparticles [18] or homogeneous like a coordination complex and enzyme.

Electrocatalytic energy conversion utilizing renewable power sources (e.g. solar and wind energy) is regarded as one of the most efficient and cleanest energy conversion pathways [19–22]. Furthermore, the converted energy is easy to store and use as clean energy or chemical stock. Specifically, the involvement of the electrocatalytic hydrogen evolution reaction (HER) in the cathode and the oxygen evolution reaction (OER) in the anode can efficiently drive water splitting and finally convert the electrical energy into chemical form, that is, hydrogen energy [23–25].

Hopely this review will be useful in identifying the best synthesis and characterization technique, factors affecting the performance and the potential applications of two-dimensional for the future.

II. Synthesis of Two-dimensional Materials

Two-dimensional materials can be syntheses using two main approaches namely:

a) Top-Down Approach
b) Bottom-Up approach

A. Top-Down Approach

This approach consists of mechanical exfoliation and chemical exfoliation.

Mechanical Exfoliation: Mechanical exfoliation is to prepare monolayer or few-layer two-dimensional (2D) materials by applying an adhesive tape to cleave bulk crystals repeatedly as also known as 'Scotch tape method' (figure 2.1). This simple mechanical cleavage method has been used to successfully obtain a variety of two-dimensional (2D) layered materials such as graphene, boron nitride, dichalcogenides, and so on [26]. The prepared layered materials exhibit high crystallinity and clean surfaces, making them attractive for fundamental research. However, the obvious disadvantage of extremely low yield restricts its large-scale production and applications. Most layered materials have relatively weak bonds such as van der Waals, or hydrogen holding the layers together. It follows that two-dimensional (2D) layers can be readily exfoliated from three-dimensional (3D) crystals mechanically by cleaving the crystals against another surface. Novoselov et. al. [27] were the first to use this approach to separate single graphene layers from highly oriented pyrolytic graphite (HOPG), using Scotch tape to peel the graphene layers which then were transferred to a Si wafer for extensive investigation. This approach enabled Novoselov et. al. [27] to investigate the electronic behavior of single layers of graphene for the first time. Another mechanical method entails rubbing the three-dimensional (3D) materials against paper like writing with chalk on a blackboard or writing with a graphite pencil on paper [28]. Mechanical exfoliation was extended to many layered materials other than graphene including: h-BN, [28, 29] TMDs, [28, 30] MoO3, [31, 32] and hydrated WO3 [33].

Figure 2.1: Scotch tape used for mechanical exfoliation [27]

The general procedure of mechanical exfoliation using Scotch tape is divided into two parts. The first step is to thin down the bulk materials by putting them onto the Scotch tape and peeling off repeatedly until the thick bulk materials are thinned down to some degree as shown in Figure 2.3. The second step is to transfer the exfoliated flakes on the tape to the surface of a substrate by sticking the tape on the substrate. A few finished samples are shown in Figure 2.3 and 2.4. After the transferring of the flakes, optical inspection is used to identify the suitable flakes for the subsequent material characterization and device fabrication [34].

As can be seen in Figure 2.3, there are built-in alignment marks in the form of numbers and squares on the substrate, circled in red together with the material flakes. Since the flakes in various shapes are transferred and then distributed on the surface of substrates in a random order, the alignment marks are needed to record the location of the desirable flakes for the subsequent processing. The period of the alignment mark arrays is 76μm and they are repeated over the entire surface of the substrates. The numbers indicate the row and column of the alignment marks respectively. For example, the numbers of 30 and 29 in Figure 2.3 surrounded by four square marks indicate the column number is 30 and row number is 29 [34].

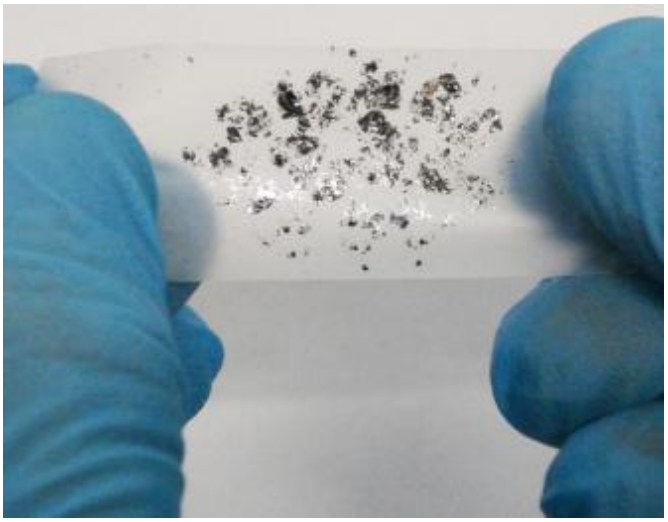

Figure 2.2: Material flakes on scotch tape [34]

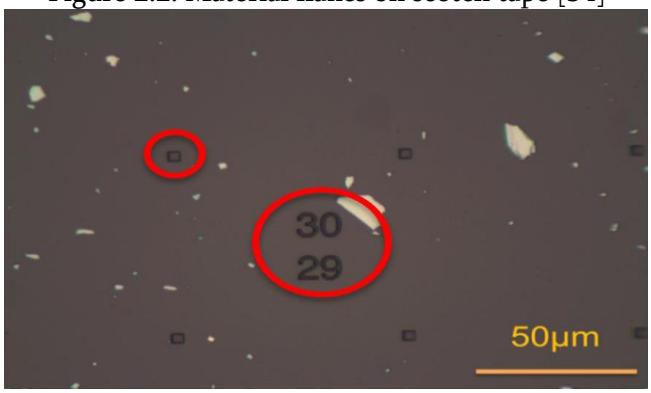

Figure 2.3: An optical image of a Si wafer with alignment marks (circled in red) and randomly distributed material flakes in top view [34].

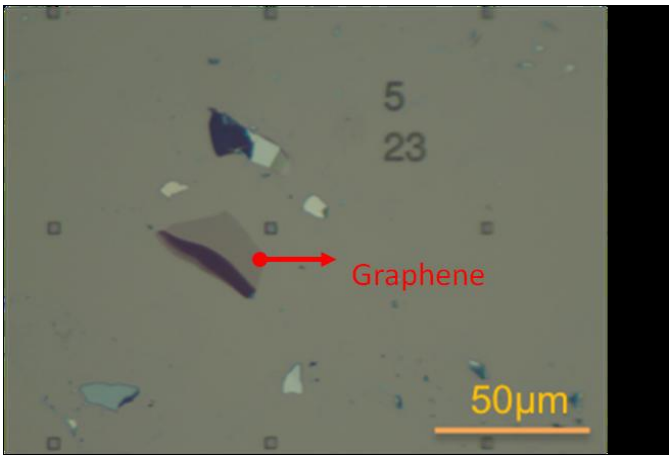

(a)

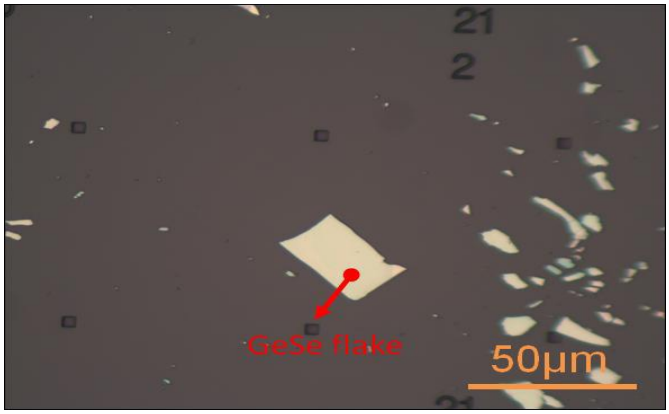

(b)

Figure 2.4 Optical images of (a) graphene sheet and (b) thin GeSe sheet on SiO_2/Si substrates obtained by the improved mechanical exfoliation [34].

Chemical Exfoliation: The main idea behind chemical exfoliation is to break the bonds between the layers by chemical, chemical-thermal (thermal treatment after chemical reaction), or chemical mechanical (chemical reaction assisted by sonication) procedures. Most of the chemical exfoliations processes are carried out in liquids. A schematic for the different liquid exfoliation mechanisms is shown in Figure 2.5 [35]. Chemical exfoliation is used for the production of a wide range of two-dimensional (2D) materials chemistries, as varied as graphene and its oxide [36-39], metal oxides and hydroxides [40-44], h-BN [45-46], TMDs [46-48] and clays [49-53].

In chemical exfoliation, solvent-assisted exfoliation and ion intercalation assisted exfoliation are two typical approaches. Solvent-assisted exfoliation was proposed by Coleman et al. in 2011 [47]. Many two-dimensional (2D) layered materials (such as MoS2, WS2, MoSe2, MoTe2, BN, Bi2Te3, and so on) could be exfoliated from the bulk crystal counterparts by direct sonication in organic solvents like N-methylpyrrolidone (NMP) and isopropanol (IPA) [53]. For the solvent assistance exfoliation process, selecting an appropriate solvent with a specific surface tension is critical because the energy of exfoliation could be minimized when the surface energies of flake and solvent match well; therefore, an effective exfoliation could be successfully achieved [47]. Generally, solvents with the specific surface tension of ~40 mJ/m2 are suitable for many materials (such as BN, MoS2, and WS2). Chemical modification of the interlayer composition is needed in some conditions where the bonds between the layers are too strong to be broken with the approaches described above [54-56]. An example of this approach is the modification of the perovskite structure KCa2Nb3O10 by proton exchanging in 2M HNO3 and then reacting with tetra (n-butyl) ammonium hydroxide (TBA+OH-) to form TBAβH1-βCa2Nb3O10 which is then easily exfoliated [54]. Sublimation of silicon from silicon carbide, SiC, single crystals by heating it under high vacuum (~ 1.3 x10-4 Pa) [57] or under argon results in forming grapheme [58]. It is worth noting that in parallel to Novoselov et al. [27] early work (the work that got them Nobel Prize in physics 2010) Berger et al.[59] used SiC to produce few-layers graphene, and they explored their electronic properties, but their paper got published about 6 weeks after Novoselov's.

The most widely used method entails, intercalating of a material or compound between the layers that ultimately results in their separation from each other. An example for that approach is intercalating potassium, K, between the graphene layers then exposing the potassium intercalated graphite to water or ethanol [60]. The vigorous reaction between the intercalated K and water results in separating the graphene layers from each other.

Another example is the reaction of graphite with a mixture of acids (nitric acid, and sulfuric acid) with potassium chlorate, which results in oxidizing the graphite. Then by thermal shock (rapid heating to 1050 °C for 30 s) the intercalant decompose with a large volume expansion those results in separating the two-dimensional (2D) graphene oxide layers from each other [61].

Sonication assisted exfoliation can also be used instead of thermal shock to exfoliate the intercalated graphene oxide layers [62]. Exfoliation of TMDs can be carried out by sonicating their powders in different solvents such as N-methyl-pyrrolidone or isopropanol [46]. Similarly, graphene sheets can be exfoliated by sonication in water with additives of surfactants [63]. As shown in Figure 2.5c, using the right solvent is very important to avoid restacking and re-agglomeration [46].

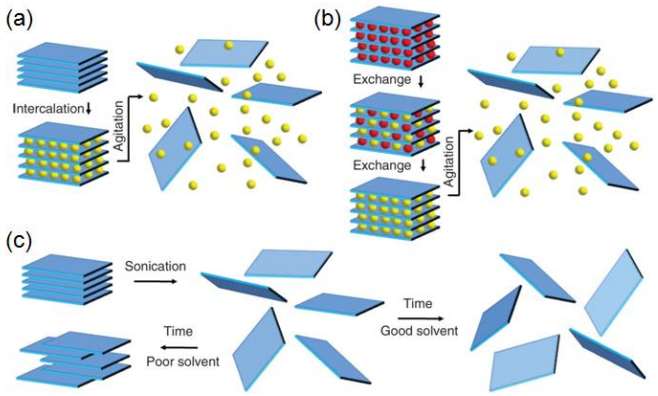

Figure 2.5: Schematic for the different liquid exfoliation mechanisms (a) Intercalation followed by agitation, (b) chemical modification by exchanging the compound that is between the layers by other intercalants followed by agitation, and, (c) sonication, if carried out in the right solvent, the sonicated layers will stay in suspension for a long time, if not the layers will restack [35].

A. *Bottom-up Approach*

The main techniques that use a bottom-up approach to synthesis 2D materials are chemical vapor deposition, CVD and physical vapor deposition, PVD.

Chemical Vapor Deposition (CVD): This involves chemical reactions of gaseous reactants on a heated substrate surface [64-65]. The CVD approach has been used successfully in synthesizing 1T-VS_2 [66, 67], 1T-VSe_2 [68, 69], 2H-NbS_2 [70], 3R-NbS_2 [70], 2H-$NbSe_2$ [71], 1T-TaS_2 [72, 73], 1T-$TiSe_2$ [74], and so on. Contamination-free and high crystalline quality samples with potential for scaling-up are the great advantages of the CVD method [75]. W. Fu *et al.* reported the controlled synthesis of atomically-thin 1T-TaS_2 [72] (Figure 2.6).

The tantalum pentachloride ($TaCl_5$) and sulfur (S) powder were used as precursors. As the carrier gas, a mixture of N_2 with 10% of H_2 was used. The reaction was usually carried out at 820 °C. In CVD synthesis, the system pressure, gas flow rate, precursor concentration, vaporization temperature of precursors, reaction temperature and deposition time play the key roles in controlling the quality of the crystals.

The main advantage of CVD 2D layers over mechanical or chemical exfoliation is the larger areas obtained by the former [76]. Bae *et al.* [75] reported on roll-to-roll production of more than 76 cm (30 inch screen size) graphene films for use as transparent electrodes. In principle, CVD also allows for the fabrication of electronic devices such as transistors [77].

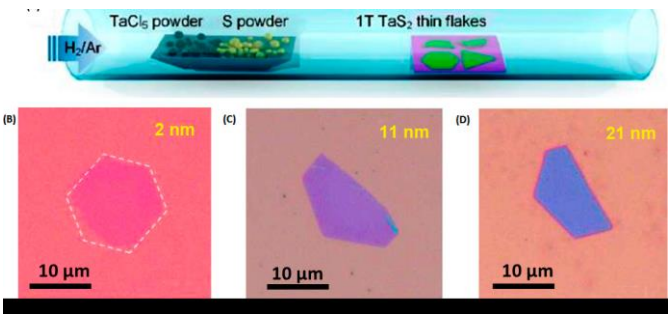

Figure 2.6: (A) Illustration of CVD growth of 1T-TaS_2 crystals using $TaCl_5$ and S as precursors. (B–D) Optical images of the as-prepared 1T-TaS_2 crystals of different thicknesses [72].

Physical Vapor Deposition (PVD): Physical vapor deposition approach is to obtain two-dimensional (2D) materials by recrystallisation of materials through a vapor-solid process. Various two-dimensional (2D) materials can be prepared by PVD process. Taking In_2Se_3 as an example, Lin *et al.* [78] first reported the synthesis of atomically thin In_2Se_3 flakes with this method. By using In_2Se_3 powders as the precursor and graphene as the substrates, orientation-defined In_2Se_3 flakes with the thickness less than three layers could be achieved under the negative pressure (50 Torr). By controlling the cooling rate during the growth process, the crystalline phases of as obtained In_2Se_3 could be adjusted. Zhou *et al.* [79] later reported the preparation of the high-quality monolayer α- In_2Se_3 material by PVD method under atmospheric pressure and observed the Raman and PL signals in monolayer In_2Se_3 for the first time (Figure 2.7). However, the random nucleation of the crystals in PVD can make the layer thickness uneven, which requires more research efforts to resolve the issue. Growing 2D layers from solutions can be considered as another bottom-up approach [83]. However, the resulted 2D materials are more close to those produced by top-down approaches [84].

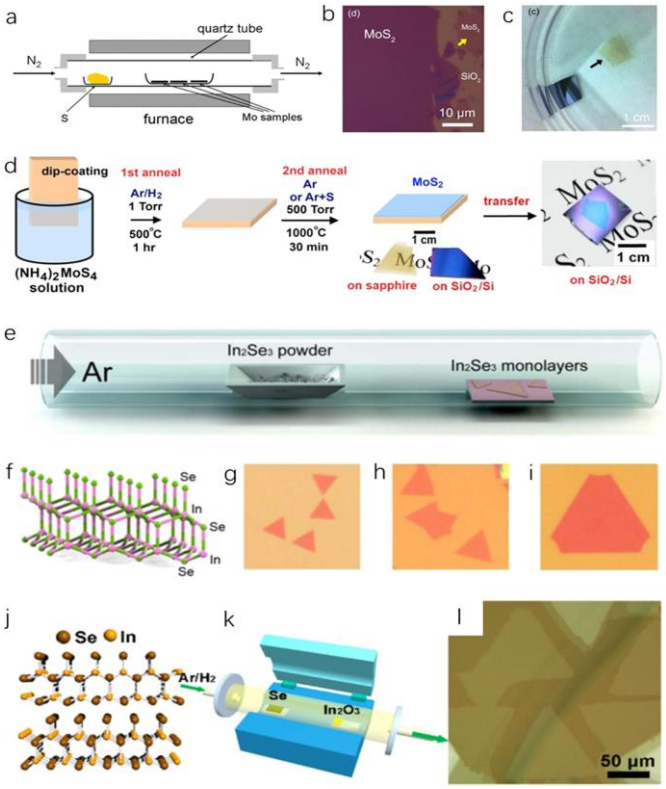

Figure 2.7: Vapor Phase Deposition Growth of 2D materials. (A-C) Synthesis of MoS_2 by selenization of Mo thin film. (A) Schematic illustration of meta-transformation for MoS_2 film preparation. (B) Optical image of MoS_2 on SiO_2/Si substrate. (C) SiO_2/Si substrate (left) and peeled off few layer Mo (right) [80]. (D) Schematic illustration of the thermal decomposition of $(NH_4)_2MoS_4$ for the synthesis of MoS_2 thin layers on insulating substrates [81]. (E-I) Synthesis of 2D In_2Se_3 flakes by PVD method. (E) Schematic illustration of PVD process for In_2Se_3 layers with In_2Se_3 powders as precursors. (F) Crystal structure of In_2Se_3 monolayer. (G-I) Optical images of In_2Se_3 with the growth time of 5, 10, and 15 min, respectively. The scale bar is 5, 10, and 10 μm, respectively [79]. (J-L) Synthesis of 2D In_2Se_3 flakes by CVD method. (J) Crystal structure of α-In_2Se_3. (K) Schematic illustration of the CVD growth process of 2D In_2Se_3 on mica substrates. (L) Optical microscope image of as-grown triangular In_2Se_3 nanosheets on mica substrate [82].

III. Characterization Techniques of Two-Dimensional (2D) Materials

A. *Raman Spectroscopic Technique*

Raman spectroscopy is a powerful tool to understand the vibrational properties of two-dimensional (2D) materials; it's also based on temperature-dependent. Recently, Raman spectra (temperature-dependent) of 1T-VSe_2 [85], 1T-TaS_2 [86], 1T-$TaSe_2$ [87], 2H-$TaSe_2$ [88, 89], 1T-$TiSe_2$ [90] and 2H-$NbSe_2$ [91] have been reported. In addition, Raman spectroscopy has been used

vastly to investigate stacking order [92, 93], number of layers [94], molecular doping [95], edge orientations [96, 97], strain effects [98, 99] and other properties of two-dimensional (2D) materials. Raman spectroscopy provides a quick, convenient, nondestructive and noninvasive method for characterizing the 2D materials with high selectively for the interior layers [100-102, 104]. Measurements can be made at room temperature and at ambient pressure without complicated sample preparation processes. Raman scattering involves the inelastic scattering of the incident light in a material, where the energy of the scattered light either decreases by exciting an elementary excitation of the solid material (i.e. a phonon) or increases by absorbing a phonon.

More accurately, Raman spectroscopy can also be used to determine the number of layers of 2D TMDs. Since the Raman spectrum provides vibrational information of the phonon structure specific to molecules which have unique Raman peaks in Raman spectra, it is used as a fingerprint to identify the molecule and an effective and quick technique to differentiate one from others. Two Raman peaks are observed in various thicknesses of MoS_2. One corresponds to in-plane E^1_{2g} mode, located at 384 cm^{-1} and the other out-plane A_{1g} mode, located at 408 cm^{-1}. And the exact positions of E^1_{2g} mode and A_{1g} mode are functions of MoS_2 film thickness. As the MoS_2 film thickness increases, E^1_{2g} mode decreases but A_{1g} mode shifts in an opposite direction, which originates from the effective restoring forces and long-range Coulomb interactions [103]. The noticeable shifts of E^1_{2g} mode and A_{1g} mode make the Raman spectra an excellent indicator of thickness in MoS_2 film, which also applies to other 2D TMDs, such as WS_2, $MoSe_2$, etc.

Raman spectra give the intensity of the scattered light as a function of the energy shift from the incident light (Raman shift). The typical accuracy of measurements of Raman spectra is 1 cm^{-1} (~0.1 meV) which is sufficient for measuring the interlayer interaction (several meV) of TMDs. Raman spectroscopy has been widely used and has become a standard characterization technique for TMDs, graphene and other atomic layer materials [101].

There are several advantages of using Raman spectroscopy for the characterization of low dimensional materials, including 2D TMDs [104, 105]. One reason is that the electronic density of states (DOS) has a so-called van Hove singularity [107], which leads to a strong Raman feature when the photon energy is matched to the van Hove singularity of the DOS for each layer.

The second advantage is that more specific selection rules predicted from the group theory applicable to the particular optical transition can be applied to many TMD layered materials with lower symmetry compared to graphene. In this way, differences in symmetry distinguish the spectral features of a particular TMD layer from another.

In addition, in the optical transitions involved in the Raman process, the optical dipole selection rule restricts the possible electronic transitions and the possible Raman-active phonon modes, which could be sensitive to the number of atomic

layers and to the laser polarization direction [106, 107].

B. *Temperature-Dependent Resistivity and Magnetic Susceptibility*

As the temperature changes, an unusual response in resistivity and magnetic susceptibility has been observed in two-dimensional (2D) material such as 1T-VS_2 [116], 1T-VSe_2 [73, 109, 110], 1T-TaS_2 [107, 112, 113] and 1T-$TaSe_2$ [114] which is also an indication of two-dimensional CDW transition. The thickness plays an important role in the CDW phase transition of 2D CDW materials.

The thickness dependence of the NC-CDW to C-CDW phase transition temperature in 1T-TaS_2 thin flakes had been reported by M. Yoshida et al. for the first time [115]. The dimensionality effect on CDW states in 1T-TaS_2 was analyzed by investigating pristine thin flakes by changing the thicknesses up to 2 nm approximately [116, 117]. It was demonstrated that both C-CDW/NC-CDW and NC-CDW/IC-CDW phase transitions are dynamically regulated for varying the sample thickness.

In contrast to 1T-TaS_2 and 1T-VSe_2, it is also reported that the CDW phase transition temperature can increase in the thinner materials. For instance, the liquid-exfoliated 4–8 layer-thick 1T-VSe_2 sample shows the CDW phase transition temperature at 135 K, whereas the bulk sample shows it at 107 K [117]. A similar phenomenon has been observed from mechanically-exfoliated $TiSe_2$ samples, where the transition temperature increases from 200–240 K, while thinning the thickness from the bulk to a few nanometers [96]. Moreover, X. Xi et al. reported the strongly enhanced CDW order in atomically-thin $NbSe_2$ TCDW > 100 K for the exfoliated monolayer sample [118], while M. Ugeda et al. observed slightly weakened CDW order (TCDW approximately 25 K) in the single layer $NbSe_2$ grown on graphene by the MBE method [119]. These dissimilarities of the transition temperature still are not well understood. The sample quality, substrates and the fabricated device status could play crucial roles in CDW phase transitions.

C. *X-Ray Diffraction Technique*

X-ray Diffraction (XRD) both small-angle X-ray scattering (SAXS) and wide-angle XRD can supply information about the unit cell structure and constituents, the sheet thickness and lateral dimensions, and the arrangement of restacked nanosheets. SAXS provides information about inter-nanosheet stacking since these peaks occur at lower angles [120]. By simulating the SAXS pattern, the stacking direction, sheet thickness, and distance between the sheets (from ligands or absorbed molecules) can be determined. For instance, patterns of wet colloidal aggregates of nanosheets and dried aggregates of nanosheets will display different XRD patterns: layer-to-layer registry can be disturbed for wet colloidal aggregates, while in-plane lattice planes are maintained, suggesting isolated nanosheets [121, 122]. For dried nanosheets, the presence of low-angle basal reflections in the pattern indicates an ordered arrangement of restacked nanosheets along the stacking axis, and likewise, the absence of intense basal reflections indicates random orientations for aggregated nanosheets [121]. The orientation of films on substrates favors the alignment of the thin axis. Broadening signatures of specific peaks under this orientation can

indicate the thin axis [122]. To gain more insight, the nanosheet XRD pattern can be modeled by the structure factor, the Lorentz polarization factor, the Laue interference function, and the temperature factor [123]. Structure factors for single and multiple layers can be calculated assuming atomic positions, unit cell structure, and orientation to a substrate [124]. Results of this modeling can help determine the fundamental units of the nanosheets (e.g., atomic make up of termination layers), the spacing between sheets, and if the nanosheets are restacked. In plane XRD can be used successfully to observe *'hk'* reflections (if l is the thickness axis) of the nanosheets' 2D unit cell [125]. This is a useful method to observe missing peaks from the naturally textured orientation of nanosheets on a substrate. Unit cell parameters can be extracted from refinements of these data and compared to bulk values.

D. *Scanning Tunneling Microscopic Technique*

Scanning Tunneling Microscopy (STM) is a probe-based technique that can measure the electronic and topographic structure of single-atom-thick materials and can manipulate single atoms at specific points in order to build and characterize nanostructures that are well isolated from the substrate [126].

Atomic arrangement in 2D materials regulates the electronic structures. Scanning Tunneling Microscopy (STM) imaging and scanning tunneling spectroscopy (STS) measurement are direct ways to reveal the atomic structure and the energy gap of 2D materials. M. M. Ugeda et al. [119] reported Scanning Tunneling Microscopy (STM) measurements on ultrathin film of 2H-$NbSe_2$. A three by three CDW structure in $NbSe_2$ has been observed. Superconductivity also remains in the 2D limit, but the transition temperature is lowered to 1.9 K (7.2 K for the bulk material).

Another examples include Scanning Tunneling Microscopy (STM) studies of the unusual cyclotron quantization in graphene [127, 128] as well as characterization of MoS_2 nanoislands [129] and BN [130] Recent focus has shifted toward studies of adsorbates and defects, including metal adatoms on graphene [131, 132] and h-BN [133, 134] and molecules on MoS_2 [135].

Other characterization techniques are Scanning Transmission Electron Microscopy (STEM) [136], Transmission Electron Microscopy (TEM) [137], Fluorescence Quenching Microscopy (FQM) [126], Scanning Electron Microscopy (SEM) [84], and so on.

1. Potential Applications of Two-Dimension (2D) Materials

Two-dimensional materials are newly developed materials with better performance evaluations and widely applications. This section will gives some of potential applications of two-dimensional materials.

E. *Catalytic Activity*

Ma et al. [138] found that Al-doped graphene-like Zinc Oxide (g-ZnO) mono-layers in which Al atoms substitute host Zn atoms show good catalytic activity for CO oxidation via the Eley–Rideal mechanism with a two-step route. In this mechanism, the first CO molecule directly interacts with the pre-adsorbed O_2 molecule, forming a carbonate-like CO_3 complex as an

intermediate state. This process is exothermic by 3.93 eV and the reaction requires only a small barrier of 0.006 eV to be overcome. The second CO molecule initially adsorbed on top of one Zn atom near the doped Al atom then approaches the CO_3 complex to form two CO_2 molecules with an energy barrier of 0.79 eV. Two CO_2 molecules are produced with adsorption energy of 0.46 eV with respect to two free CO_2 molecules in the gas phase. Since the energy released in this step (0.79 eV) can easily surmount the adsorption energy, these two CO_2 molecules can be released rather easily from the g-ZnO sheet. The reaction proceeds rapidly at low temperature, suggesting that Al-doped g-ZnO mono-layers could be an efficient catalyst for CO oxidation at low temperature.

A. Absorption of Oxide of Carbon

Rao et al. [139] investigated the interaction of CO_2 with pristine, defective and non-metal-doped graphene-like Zinc Oxide (g-ZnO) mono-layers in terms of their efficiency to capture CO_2 and hence their potential for cleaning our atmosphere and purifying fuel engine emissions. The calculated results show that a CO_2 molecule favors adsorption on the top of an O location and favors a horizontal alignment with respect to the pristine g-ZnO mono-layer (ML). The adsorption energy of the CO_2 molecule on a g-ZnO mono-layer is found to be -0.20 eV, indicating physisorption with a CO_2–gZnO distance of 2.92 Å. The CO_2 adsorption on defective as well as non-metal (B, C, N), substitutionally doped g-ZnO mono-layers was also investigated. The adsorption of CO_2 at oxygen and zinc vacancies was explored in the study on defective g-ZnO. The adsorption energy of CO_2 increases to -1.77 eV, -1.33 eV and -0.80 eV with adsorption distances of 1.53 Å, 1.44 Å and 1.41 Å for B, C and N atoms, respectively. This indicates a chemisorption mechanism with a large binding energy and a short adsorption distance and stands in contrast with physisorption on pristine g-ZnO.

In another research, Zhang et al. [140] have reported that doped g-ZnO exhibits strong chemisorption of the CO molecule by forming A-CO (where A=B, N or C dopants) in contrast to weak physisorption on pristine g-ZnO. The adsorbed CO slightly pulls the A atom out of the sheet plane, viz. the A site is transformed from sp^2 hybridization to a more sp^3-like hybridization. Total charge density calculations show that large charge transfer occurs between the doped g-ZnO and a CO molecule, while little charge is transferred between pristine g-ZnO and a CO molecule. Moreover, the shorter bond lengths of A–CO (1.43 Å, 1.24 Å, 1.32 Å for B, N and C, respectively, as compared to pristine g-ZnO, 2.32 Å) and a higher binding energy (-4.05, -2.77, -5.65 eV for B, N and C, respectively, as compared to pristine g-ZnO -0.35 eV) clearly indicate that a chemical bond can form during the adsorption process.

B. Energy Storage and Harvesting

The energy harvesting cells based on 2D piezoelectric materials are crucial for future wireless nanosystems without power supply, such as environmental monitors, implantable medical sensors, and personal electronics [141]. In 2014, Wu et al. [142] pioneered a monolayer MoS_2 as prototype nanogenerator for scavenging the mechanical energy. As for this nanogenerator, it will generate a peak voltage or current signal only during the moment of stretching and

releasing. With the increasing tensile strain, both the peak voltage and current increase. Furthermore, this type of device can still maintain a stable output even after three hours of fatigue test, demonstrating its excellent performance for harvesting various tiny mechanical vibration energies. Enlightened by this work, Lee et al. [143] developed a monolayer WSe_2 piezoelectric nanogenerator, which gives a peak voltage of 45 mV under a strain of 0.39 %. In their work, to enhance the piezoelectric outputs, CVD synthesized monolayer WSe_2 samples have been successfully transferred to the top of another one to form a special-orientated artificial bilayer (AA stacking), which could retain the piezoelectric effect, unlike its natural or pristine form. The piezoelectric coefficient for artificial bilayer can be about two times larger than that of the monolayer flakes.

Phosphorene has been considered for other electrochemical energy storage applications, such as all solid- state supercapacitors [144] and Sodium ion batteries (NaIBs), [145] which are considered safer than LIBs and use more abundant Sodium ions. The promise of using phosphorene for NaIB anode materials comes from the fact that, unlike the traditional, carbon-based anode materials for LIBs, it can accommodate Na ions, which are significantly larger than Li ions (2.04 vs. 1.52 Å). Because of this, BP with its larger interlayer channel size (3.08 vs. 1.86 Å for graphite) is a highly promising NaIB anode material with a theoretical specific capacity of ~2600 mAh g^{-1}, which dwarfs that of any other present materials.

C. Electronics and Sensing Devices

Generally, two-dimensional (2D) materials could be an ideal choice for future flexible electronics. They have excellent mechanical properties [146, 147], can be compatible with flexible device fabrication, and unlike CNTs [148, 149] do not require any sorting process [150]. At the same time, the mobility of 2DMs, when grown over large areas by CVD, can be larger than some of the organic semiconductors [151], thus enabling higher frequency at low power. For transparent conductors, graphene high conductivity and low broadband absorption makes it a promising flexible replacement for the current leading material, indium tin oxide, which is inflexible and increasingly expensive. The large variety of two-dimensional (2D) materials provides a wide selection to choose for device optimization.

Optoelectronic devices (photodetectors, solar cells and LEDs etc.) are electric devices that can generate, detect, and interact with light. Due to a large area/volume ratio, strong light–matter interaction and novel electrical properties, optoelectronic devices based on two-dimensional (2D) materials have attracted much interest since the beginning.

The direct band gaps of monolayer TMDs make them attractive as light-absorbing materials in alternative thin-film solar cells, including flexible photovoltaics that could coat buildings and curved structures. The first trial was on MoS_2 [152]. This was inspired by the finding that MoS_2 has a direct band gap of about 1.8 eV when its thickness is reduced to a single layer. In 2013, Lopez-Sanchez et al. conducted a landmark research [153]. They reduced charged impurities scattering and contact resistance by the careful treatment on a dielectric layer and an annealing process. After these processes, an impressive high

responsivity of 880 AW^{-1} was achieved. Stimulated by the pioneering works on MoS_2, photo-detectors based on other TMDs, like $MoSe_2$, WS_2 and WSe_2, have attracted growing attention in recent years [154–156]. In addition, combining different 2-D materials together to form heterostructures may be a possible solution [157, 158].

D. CO_2 reduction

Li et al. [159] reported amorphous MoS_2 on a polyethylenimine-modified reduced graphene oxide substrate as an effective catalyst for electrocatalytic CO_2 reduction. The catalyst is capable of producing CO at an over potential as low as 140 mV and reaches a maximum Faradaic efficiency (FE) of 85.1% at an over potential of 540 mV. Another interesting point is that at an over potential of 290 mV with respect to the formation of CO, it catalyses the formation of syngas with high stability, which could be readily utilized in the current Fischer-Tropsch process and produce liquid fuels, such as ethanol and methanol. Their detailed mechanism investigation indicated that the efficiency and selectivity towards CO_2 reduction rather than hydrogen evolution at the optimal applied potential were attributed to the synergetic effect of MoS_2 and PEI:

a) The intrinsic properties of MoS_2 that it can selectively bind the intermediate during the CO_2 reduction reaction path is the principal factor contributing the CO_2 reduction and
b) PEI, an amine containing polymer with outstanding CO_2 adsorption capacity, can stabilize the intermediate and thus lower the energy barrier by hydrogen bond interaction.

Recently, Norskov et al. demonstrated theoretically that MoS_2 or $MoSe_2$ could possibly be electrocatalysts for CO_2 reduction by DFT calculation [160, 161]. Their results indicate the edge site of MoS_2 or $MoSe_2$ is active for electrochemical CO_2 reduction due to the different scaling relationships of adsorption energies between key reaction intermediates (*CO and *COOH) on the edges of MoS_2 or $MoSe_2$ compared to transition metals. Experimental results of MoS_2 as electrocatalyst for CO_2 reduction were firstly reported by Asadi et al. [162]. They uncovered that MoS_2 showed superior CO_2 reduction performance compared with the noble metals with a high current density and low over potential (54 mV) in an ionic liquid. They also utilized DFT calculations to reveal the catalytic activity mainly arises from the molybdenum-terminated edges of MoS_2 due to their metallic character and a high *d*-electron density. The experimental result that vertically aligned MoS_2 showed an enhanced performance compared to bulk MoS_2 crystal supported their calculations.

IV. Conclusion and Future Works

In conclusion, the synthesis processes, characterization techniques and potential applications of two-dimensional materials with consideration of elecrocatalysis have been discussed extensively.

Though great progress has been made, it is still far from the wide application of 2D electrocatalysis. There are still many challenges like the low yield/cost efficiency, degradation,

kinetics of charge transfer and trap, and recycling. The recycling problem may be resolved by designing suitable devices or tuning the magnetic properties, but the efficiency and robustness can only count on the development of more advanced materials.

The 2D material family offers a new class of materials characterized by strong covalent bonds in-plane but only very weak Van der Waal's coupling between the layers, leading to a material system with almost ideally self-passivated structures.

The most promising applications of 2D materials must be developed based on the unique properties of this material system that are not often found in other materials. 2D materials offer three key properties that are particularly attractive for future applications: the flexibility and transparency, the ease for heterogeneous integration without lattice mismatch problem, and extraordinary sensing capability due to high surface-to-volume ratio and high mobility.

The first area is to develop 2D materials for GHz frequency ubiquitous electronics applications.

A second promising application of 2D materials lies in their outstanding optical properties. Optoelectronics devices, such as photodetectors, LEDs and even lasers, based on 2D materials can be envisioned to emerge where they can be placed on to arbitrary surfaces including flexible and transparent ones. New opportunities can arise in developing THz and infrared sensors based on graphene either based on conventional device structure or novel plasmonic devices. Low cost solar cells to be placed on any type of substrates can also be developed where many potential applications exist, for example as the energy harvesting units in self-powered sensors or sensor networks.

2D materials like graphene are very attractive bio-compatible options of flexible and semitransparent electrodes for interfacing with the brain neurons. 2D materials can also be used to build low-cost biosensors with many potential applications, such as glucose detection, moisture sensing, and body temperature monitoring.

V. REFERENCES

1. Fengwang Li and Mianqi Xue (2016). Two-Dimensional Transition Metal Dichalcogenides for Electrocatalytic Energy Conversion Applications, retrieved from http://dx.doi.org/10.5772/63947
2. Novoselov KS, Geim AK, Morozov S, Jiang D, Zhang Y, Dubonos Sa (2004). Electric field effect in atomically thin carbon films. Science; 306:666-669.
3. Mueller, T., Xia, F. & Avouris, P. (2010). Graphene photodetectors for high-speed optical communications. Nat. Photon. 4, 297-301.
4. Liu, Y. (2011). Plasmon resonance enhanced multicolour photodetection by graphene. Nat. Commun. 2, 579.
5. Applied Graphene Materials plc: Graphene dispersions Retrieved from http://www.appliedgraphenematerials.com
6. Hu Guohua, Kang Joohoon, Ng Leonard W. T, Zhu Xiaoxi, Howe Richard C. T., John Christopher G., Hersam Mark C., Hasan Tawfique (2018). Functional inks and printing of two-dimensional materials. Chemical Society Reviews. 47(9), pp: 3265-3300.
7. Kerativitayanan P., Carrow J. K., Gaharwar A. K., (2015). Nanomaterials for Engineering Stem

Cell Responses. Advanced Healthcare Materials. 4(11), pp: 1600-1627.

8. Gaharwar A. K., Peppas N. A., Khademhosseini A., (2014). Nanocomposite hydrogels for biomedical applications. Biotechnology and Bioengineering. 111(3), pp: 441-453.
9. Chhowalla M., Shin H. S., Eda G., Li L. J., Loh K. P., Zhang H. (2013). The chemistry of two-dimensional layered transition metal dichalcogenide nanosheets. Nature Chemistry; 5:263-275.
10. Das S., Robinson J. A., Dubey M., Terrones H., Terrones M. (2015). Beyond graphene: progress in novel two-dimensional materials and van der Waals solids. Annual Review of Materials Research; 45:1-27.
11. Sun Y, Gao S, Lei F, Xie Y. (2015). Atomically-thin two-dimensional sheets for understanding active sites in catalysis. Chemical Society Reviews; 44:623-636.
12. Wang Z, Zhu W, Qiu Y, Yi X, von dem Bussche A, Kane A, et al. (2016). Biological and environmental interactions of emerging two-dimensional nanomaterials. Chemical Society Reviews; 45:1750-1780.
13. Zhang X & Xie Y. (2013). Recent advances in free-standing two-dimensional crystals with atomic thickness: design, assembly and transfer strategies. Chemical Society Reviews; 42:8187-8199.
14. Luo B, Liu G, Wang L. (2016). Recent advances in 2D materials for photocatalysis. Nanoscale; 8:6904-6920. DOI: 10.1039/c6nr00546b.
15. Garcia J. C., De Lima D. B., Assali L. V. C., Justo J. F., (1324). Group IV grapheme and graphene-like nanosheets. Journal of Physical Chemistry C. 115(27), pp: 13242-13246.
16. Lei Yang, Ping Liu, Jing Li and Bin Xiang (2017). Two-Dimensional Material Molybdenum Disulfides as Electrocatalysts for Hydrogen Evolution. Catalysts, 7, 285; pp 1-18, doi:10.3390/catal7100285. Retrieved from www.mdpi.com/journal/catalysts
17. Valenti G., Boni A., Melchionna M., Cargnello M., Nasi L., Bertoli G., Gorte R. J., Marcaccio M., Rapino S., Bonchio M., Fornasiero P., Prato M., Paolucci F. (2016). Co-axial Heterostructures Integrating Palladium/Titanium-dioxide with Carbon Nanotubes for Efficient Electrocatalytic Hydrogen Evolution. Nature Communications. 7: 13549.
18. Wang Xin (2018).CNTs tuned to provide electrocatalyst support. Retrieved from http://www.nanotechweb.org
19. Hong W. T., Risch M., Stoerzinger K. A., Grimaud A., Suntivich J., Shao-Horn Y. (2015). Toward the rational design of non-precious transition metal oxides for oxygen electrocatalysis. Energy and Environmental Science; 8, pp:1404-1427.
20. Bonaccorso F., Colombo L., Yu G., Stoller M., Tozzini V., Ferrari A. C., (2015). Two-dimensional (2D) materials. Graphene, related two-dimensional crystals, and hybrid systems for energy conversion and storage. Science; 347:1246501.
21. Xie J., & Xie Y. (2015). Transition metal nitrides for electrocatalytic energy conversion: opportunities and challenges. Chemistry - A European Journal; 22, pp: 3588-3598.
22. Zhang G., Liu H., Qu J., Li J. (2016). Two-dimensional layered MoS2: rational design, properties and electrochemical applications. Energy and Environmental Science; 9, pp; 1190-1209. DOI: 10.1039/c5ee03761a.
23. Mallouk T. E. (2013). Water electrolysis: divide and conquer. Nature Chemistry; 5, pp: 362-363.
24. Turner J. A. (2004). Sustainable hydrogen production. Science; 305, pp: 972-974.
25. Norskov J. K., & Christensen C. H. (2006). Toward efficient hydrogen production at surfaces. Science; 312, pp: 1322-1323.
26. Novoselov, K. S., Jiang, D., Schedin, F., Booth, T. J., Khotkevich, V. V., Morozov, S. V., & Geim, A. K. (2005). Two-dimensional atomic crystals. Proceeding National Acadamic Science. USA 102, pp: 10451-10453.
27. K. S. Novoselov, A. K. Geim, S. V. Morozov, D. Jiang, Y. Zhang, S. V. Dubonos, I. V. Grigorieva, A. A. Firsov (2004), Science, 306, 666.
28. D. Pacil, J. C. Meyer,. Girit, A. Zettl, (2008). Applied Physics Letters, 92.

29. H. Li, G. Lu, Y. Wang, Z. Yin, C. Cong, Q. He, L. Wang, F. Ding, T. Yu, H. Zhang, (2013). Small, 9, 1974.
30. K. Kalantar-zadeh, J. Tang, M. Wang, K. L. Wang, A. Shailos, K. Galatsis, R. Kojima, V. Strong, A. Lech, W. Wlodarski, R. B. Kaner, (2010). Nanoscale, 2, 429.
31. S. Balendhran, J. Deng, J. Z. Ou, S. Walia, J. Scott, J. Tang, K. L. Wang, M. R. Field, S. Russo, S. Zhuiykov, M. S. Strano, N. Medhekar, S. Sriram, M. Bhaskaran, K. Kalantar-zadeh, (2013). Advanced Materials, 25, 109.
32. K. Kalantar-zadeh, A. Vijayaraghavan, M.-H. Ham, H. Zheng, M. Breedon, M. S. Strano, (2010). Chemistry of Materials, 22, 5660.
33. Zhengfeng Yang (2017). Electronic Device Fabrication and Characterization Based on Two-Dimensional Materials, Master of Science Thesis at University of Illinois at Urbana-Champaign.
34. V. Nicolosi, M. Chhowalla, M. G. Kanatzidis, M. S. Strano, J. N. Coleman, (2013). Science, 340.
35. Y. Hernandez, V. Nicolosi, M. Lotya, F. M. Blighe, Z. Sun, S. De, I. McGovern, B. Holland, M. Byrne, Y. K. Gun'Ko, (2008). Nature Nanotechnology, 3, 563.
36. S. Park, R. S. Ruoff, (2009). Nature Nanotechnology, 4, 217.
37. S. Stankovich, D. A. Dikin, R. D. Piner, K. A. Kohlhaas, A. Kleinhammes, Y. Jia, Y. Wu, S. T. Nguyen, R. S. Ruoff, (2007). Carbon, 45, 1558.
38. G. Eda, G. Fanchini, M. Chhowalla, (2008). Nature Nanotechnology, 3, 270.
39. R. Ma, & T. Sasaki, (2010). Advanced Materials, 22, 5082.
40. Y. Omomo, T. Sasaki, Wang, M. Watanabe, (2003). Journal of the American Chemical Society, 125, 3568.
41. R. Ma, Z. Liu, L. Li, N. Iyi, T. Sasaki, (2006). Journal of Materials Chemistry, 16, 3809.
42. L. Li, R. Ma, Y. Ebina, N. Iyi, T. Sasaki, (2005). Chemistry of Materials, 17, 4386.
43. Q. Wang, & D. OHare, (2012). Chemical Reviews, 112, 4124.
44. Y. Lin, T. V. Williams, J. W. Connell, (2009). Journal of Physical Chemistry Letters, 1, 277.
45. J. N. Coleman, M. Lotya, A. ONeill, S. D. Bergin, P. J. King, U. Khan, K. Young, A. Gaucher, S. De, R. J. Smith, I. V. Shvets, S. K. Arora, G. Stanton, H. Y. Kim, K. Lee, G. T. Kim, G. S. Duesberg, T. Hallam, J. J. Boland, J. J. Wang, J. F. Donegan, J. C. Grunlan, G. Moriarty, A. Shmeliov, R. J. Nicholls, J. M. Perkins, E. M. Grieveson, K. Theuwissen, D. W. McComb, P. D. Nellist, V. Nicolosi, (2011). Two-dimensional nanosheets produced by liquid exfoliation of layered materials. Science, 42, 568-571.
46. Z. Zeng, Z. Yin, X. Huang, H. Li, Q. He, G. Lu, F. Boey, H. Zhang, (2011). Angewandte Chemie International Edition, 50, 11093.
47. J. Feng, X. Sun, C. Wu, L. Peng, C. Lin, S. Hu, J. Yang, Y. Xie, (2011). Journal of the American Chemical Society, 133, 17832.
48. T. Lan, & T. J. Pinnavaia, (1994). Chemistry of Materials, 6, 2216.
49. J. Ma, Z.-Z. Yu, Q.-X. Zhang, X.-L. Xie, Y.-W. Two-dimensional nanosheets produced by liquid exfoliation of layered materials. Science, 42, 568-571.Mai, I. Luck, (2004). Chemistry of Materials, 16, 757.
50. M. Valkov, M. Rieder, V. Matejka, P. Capkov, A. Sliva, (2007). Applied Clay Science, 35, 108.
51. J. H. Park, S. C. Jana, (2003). Macromolecules, 36, 2758.
52. Smith, R. J. et al. (2011). Large-scale exfoliation of inorganic layered compounds in aqueous surfactant solutions. Advanced Materials, 23, 3944.
53. R. E. Schaak, T. E. Mallouk, (2000). Chemistry of Materials, 12, 2513.
54. Y.-S. Han, I. Park, J.-H. Choy (2001). Journal of Materials Chemistry, 11, 1277.
55. M. M. J. Treacy, S. B. Rice, A. J. Jacobson, J. T. Lewandowski, (1990). Chemistry of Materials, 2, 279.
56. A. J. Van Bommel, J. E. Crombeen, A. Van Tooren, (1975). Surface Science, 48, 463.
57. K. V. Emtsev, A. Bostwick, K. Horn, J. Jobst, G. L. Kellogg, L. Ley, J. L. McChesney, T. Ohta, S. A. Reshanov, J. Rhrl, (2009). Nature Materials, 8, 203.

58. C. Berger, Z. Song, T. Li, X. Li, A. Y. Ogbazghi, R. Feng, Z. Dai, A. N. Marchenkov, E. H. Conrad, P. N. First, W. A. de Heer, (2004). Journal of Physical Chemistry B, 108, 19912.
59. L. M. Viculis, J. J. Mack, O. M. Mayer, H. T. Hahn, R. B. Kaner, (2005). Journal of Materials Chemistry, 15, 974.
60. M. J. McAllister, J.-L. Li, D. H. Adamson, H. C. Schniepp, A. A. Abdala, J. Liu, M. Herrera-Alonso, D. L. Milius, R. Car, R. K. Prud'homme, I. A. Aksay, (2007). Chemistry of Materials, 19, 4396.
61. G. Wang, J. Yang, J. Park, X. Gou, B. Wang, H. Liu, J. Yao, (2008). Journal of Physical Chemistry C, 112, 8192.
62. M. Lotya, Y. Hernandez, P. J. King, R. J. Smith, V. Nicolosi, L. S. Karlsson, F. M. Blighe, S. De, Z. Wang, I. T. McGovern, G. S. Duesberg, J. N. Coleman, (2009). Journal of the American Chemical Society, 131, 3611.
63. Choy, K. L. (2003). Chemical vapour deposition of coatings. Progressive Material Science. 48, pp: 57-170.
64. Hou, X. & Choy, K. L. (2006). Processing and applications of aerosol-assisted chemical vapor deposition. Chemical Vapor Deposition, 12, pp: 583-596.
65. Yuan, J.; Wu, J.; Hardy, W.J.; Loya, P.; Lou, M.; Yang, Y.; Najmaei, S.; Jiang, M.; Qin, F.; Keyshar, K. (2015). Facile synthesis of single crystal vanadium disulfide nanosheets by chemical vapor deposition for efficient hydrogen evolution reaction. Advanced Materials, 27, pp: 5605-5609.
66. Ji, Q.; Li, C.; Wang, J.; Niu, J.; Gong, Y.; Zhang, Z.; Fang, Q.; Zhang, Y.; Shi, J.; Liao, L. (2017). Metallic vanadium disulfide nanosheets as a platform material for multi-functional electrode applications. Nano Letters, 17, pp: 4908-4916.
67. Nicolas, D. B.; Christopher, S. B.; Claire, J. C.; Ivan, P. P.; Prieto, A. G. (2007). Atmospheric pressure chemical vapour deposition of vanadium diselenide thin films. App. Surf. Sci., 253, 6041-6046.
68. Zhang, Z.; Niu, J.; Yang, P.; Gong, Y.; Ji, Q.; Shi, J.; Fang, Q.; Jiang, S.; Li, H.; Zhou, X. (2017). Van der waals epitaxial growth of 2D metallic vanadium diselenide single crystals and their extra-high electrical conductivity. Advanced Materials, 1702359.
69. Wang, X.; Lin, J.; Zhu, Y.; Luo, C.; Suenaga, K.; Cai, C.; Xie, L. (2017). Chemical vapor deposition of trigonal prismatic NbS2 monolayer and 3R-polytype few-Layers. Nanoscale, in revision.
70. Wang, H.; Huang, X.; Lin, J.; Cui, J.; Chen, Y.; Zhu, C.; Liu, F.; Zeng, Q.; Zhou, J.; Yu, P. (2017). High-quality monolayer superconductor NbSe2 grown by chemical vapour deposition. Nature. Communications, 8, 394.
71. Fu,W.; Chen, Y.; Lin, J.;Wang, X.; Zheng, Q.; Zhou, J.; Zheng, L.;Wang, H.; He, Y.; Fu, Q. (2016). Controlled synthesis of atomically thin 1T-TaS2 for tunable charge density wave phase transitions. Chem. Mater., 28, pp: 7613-7618.
72. Jin, G.; Kim, C.; Jo, H.; Kwon, S.H.; Jeong, S. J.; Lee, H. B. R.; Ahn, J. H. (2017). Vapor phase synthesis of TaS2 nanocrystals with iodine as transport agent. Japan Journal of Applied Physics, 56, 045501.
73. Boscher, N. D.; Carmalt, C. J.; Parkin, I. P. (2006). Atmospheric pressure CVD of TiSe2 thin films on glass. Chem. Vap. Deposition, 12, 54-58.
74. Bae, S.; Kim, H.; Lee, Y.; Xu, X.; Park, J.S.; Zheng, Y.; Balakrishnan, J.; Lei, T.; Kim, H. R.; Song, Y.I. (2010). Roll-to-roll production of 30-inch graphene films for transparent electrodes. Nature Nanotechnology, 5, pp: 574-578.
75. A. N. Obraztsov, (2009). Nature Nanotechnology, 4, 212.
76. M. P. Levendorf, C. S. Ruiz-Vargas, S. Garg, J. Park, (2009). Nano Letters, 9, 4479.
77. Lin, M. et al. (2013). Controlled growth of atomically thin In2Se3 flakes by van der Waals epitaxy. Journal of American Chemical Society. 135, 13274.
78. Zhou, J. et al. (2015). Controlled synthesis of high-quality monolayered a-In2Se3 via physical vapor deposition. Nano Letters. 15, 6400.
79. Zhan, Y., Liu, Z., Najmaei, S., Ajayan, P. M. & Lou, J. (2012). Large-area vapor-phase growth and characterization of MoS2 atomic layers on a SiO2 substrate. Small. 8, pp: 966-971.

80. Liu, K. K. et al. (2012). Growth of large-area and highly crystalline MoS2 thin layers on insulating substrates. Nano Letters. 12, pp: 1538-1544.
81. Feng, W. et al. (2016). Sensitive electronic-skin strain sensor array based on the patterned two-dimensional a-In2Se3. Chem. Mater. 28.
82. F. Wang, & X. Wang, (2014). Nanoscale, DOI: 10.1039/C4NR00973H.
83. Michael Naguib Abdelmalak (2014). MXenes: A New Family of Two-Dimensional Materials and its Application as Electrodes for Li-ion Batteries. Ph.D Thesis at Drexel University.
84. Sugai, S.; Murase, K.; Uchida, S.; Tanaka, S. (1981). Investigation of the charge density waves in 1T-VSe2 by Raman scattering. J. Phy. Colloques, 42, pp: 740-742.
85. Hirata, T.; Ohuchi, F.S. (2001). Temperature dependence of the Raman spectra of 1T-TaS2. Solid State. Communications, 117, pp: 361-364.
86. Samnakay, R.; Wickramaratne, D.; Pope, R.; Lake, R. K.; Salguero, T. T.; Balandin, A. A. (2015). Zone-folded phonons and the commensurate incommensurate charge-density-wave transition in 1T-TaSe2 thin films. Nano Letters, 15, pp: 2965-2973.
87. Hajiyev, P.; Cong, C.; Qiu, C.; Yu, T. (2013). Contrast and Raman spectroscopy study of single- and few-layered charge density wave material: 2H-TaSe2. Sci. Rep., 3, 2593.
88. Sugai, S.; Murase, K. (1982). Generalized electronic susceptibility and charge density waves in 2H-TaSe2 by Raman scattering. Phys. Rev. B., 25, pp: 2418-2427.
89. Goli, P.; Khan, J.; Wickramaratne, D.; Lake, R. K.; Balandin, A. A. (2012). Charge density waves in exfoliated films of Van der waals materials: Evolution of Raman spectrum in TiSe2. Nano Letters, 12, pp: 5941-5945.
90. Xi, X.; Zhao, L.; Wang, Z.; Berger, H.; Forro, L.; Shan, J.; Mak, K. F. (2015). Strongly enhanced charge-density-wave order in monolayer NbSe2. Nature Nanotechnology, 10, pp: 765-769.
91. Cong, C.; Yu, T.; Sato, K.; Shang, J.; Saito, R.; Dresselhaus, G. F.; Dresselhaus, M. S. (2011). Raman characterization of ABA-and-ABC-Stacked trilayer graphene. ACS Nano., 5, pp: 8760-8768.
92. Lui, C.H.; Li, Z.; Chen, Z.; Klimov, P. V.; Brus, L. E.; Heinz, T. F. (2011). Imaging stacking order in few-layer graphene. Nano letters, 11, pp: 164-169.
93. Li, S. L.; Miyazaki, H.; Song, H.; Kuramochi, H.; Nakaharai, S.; Tsukagoshi, K. (2012). Quantitative Raman spectrum and reliable thickness identification for atomic layers on insulating substrates. ACS Nano., 6, pp: 7381-7388.
94. Lv, R.; Li, Q.; Mndez, A. R. B.; Hayashi, T.; Wang, B.; Berkdemir, A.; Hao, Q.; Elias, A. L.; Silva, R. S.; Gutirrez, H. R. (2012). Nitrogen-doped graphene: Beyond single substitution and enhanced molecular sensing. Sci. Rep., 2, 586.
95. Cong, C.; Li, K.; Zhang, X. X.; Yu, T. (2013). Visualization of arrangements of carbon atoms in graphene layers by Raman mapping and atomic-resolution TEM. Sci. Rep., 3, 1195.
96. Cong, C.; Yu, T.; Wang, H. M. (2010). Raman study on the G-mode of graphene for determination of edge orientation. ACS Nano., 4, pp: 3175-3180.
97. Lee, J. E.; Ahn, G.; Shim, J.; Lee, Y. S.; Ryu, S. (2012). Optical separation of mechanical strain from charge doping in graphene. Nature Communications, 3, 1024.
98. Ni, Z. H.; Yu, T.; Lu, Y. H.; Wang, Y. Y.; Feng, Y. P.; Shen, Z. X. (2008). Uniaxial strain on graphene: Raman spectroscopy study and bandgap opening. ACS Nano., 2, pp: 2301-2305.
99. R. Saito, M. Hofmann, G. Dresselhaus, A. Jorio, M. S. Dresselhaus, (2011). Raman spectroscopy of graphene and carbon nanotubes. Adv. Phys. 60, pp: 413-550.
100. A. Jorio, R. Saito, G. Dresselhaus, M. S. Dresselhaus, (2011). Raman Spectroscopy in Graphene Related Systems (Wiley-VCH, 2011).
101. M. S. Dresselhaus, A. Jorio, R. Saito, (2010). Characterizing Graphene, Graphite, and Carbon Nanotubes by Raman Spectroscopy. Annu. Rev. Condens. Matter Phys. 1, pp: 89-108.
102. A. Molina-Sanchez and L. Wirtz, (2011). Phonons in single-layer and few-layer MoS2

and WS2, Physical Review B, vol. 84, pp: 155413.

103. M. S. Dresselhaus, A. Jorio, M. Hofmann, G. Dresselhaus, R. Saito, (2010). Perspectives on Carbon Nanotubes and Graphene Raman Spectroscopy. Nano Letter. 10, pp: 751-758.
104. X. Zhang, (2015). Phonon and Raman scattering of two-dimensional transition metal dichalcogenides from monolayer, multilayer to bulk material. Chem. Soc. Rev. 44, pp: 2757-2785.
105. S. Huang, (2016). In-Plane Optical Anisotropy of Layered Gallium Telluride. ACS Nano. 10, pp: 8964-8972.
106. X. Ling, (2016). Anisotropic Electron-Photon and Electron-Phonon Interactions in Black Phosphorus. Nano Letter. 16, pp: 2260-2267.
107. Mulazzi, M.; Chainani, A.; Katayama, N.; Eguchi, R.; Matsunami, M.; Ohashi, H.; Senba, Y.; Nohara, M.; Uchida, M.; Takagi, H. (2010). Absence of nesting in the charge-density-wave system 1T-VS2 as seen by photoelectron spectroscopy. Phys. Rev. 82, 075130.
108. Xu, K.; Chen, P.; Li, X.; Wu, C.; Guo, Y.; Zhao, J.; Wu, X.; Xie, Y. (2013). Ultrathin nanosheets of vanadium diselenide: A metallic two-dimensional material with ferromagnetic charge-density-wave behavior. Angew. Chem. Int. Ed., 52, pp: 10477-10481.
109. Yang, J.; Wang, W.; Liu, Y.; Du, H.; Ning, W.; Zheng, G.; Jin, C.; Han, Y.; Wang, N.; Yang, Z. (2014). Thickness dependence of the charge-density-wave transition temperature in VSe2. Appl. Phys. Lett., 105, 063109.
110. Yu, Y.; Yang, F.; Lu, X. F.; Yan, Y. J.; Cho, Y. H.; Ma, L.; Niu, X.; Kim, S.; Son, Y. W.; Feng, D. (2015). Gate-tunable phase transitions in thin flakes of 1T-TaS2. Nature Nanotechnology, 10, pp: 270-276.
111. Liu, G.; Debnath, B.; Pope, T. R.; Salguero, T. T.; Lake, R. K.; Balandin, A. A. (2016). A charge-density-wave oscillator based on an integrated tantalum disulfide-boron nitride-graphene device operating at room temperature. Nature Nanotechnology, 11, pp: 845-850.
112. Mutka, H.; Zuppiroli, L.; Molinie, P.; Bourgoin, J. C. (1981). Charge-density waves and localization in electron-irradiated 1T-TaS2. Phys. Rev. B, 23, pp: 5030-5037.
113. Wilson, J. A.; Di Salvo, F. J.; Mahajan, S. (1974). Charge-density waves in metallic, layered, transition-metal dichalcogenides. Phys. Rev. Lett., 32, pp: 882-884.
114. Yoshida, M.; Yijin, Z.; Jianting, Y.; Ryuji, S.; Yasuhiko, I.; Shigeru, K.; Akihiko, F.; Yoshihiro, I. (2014). Controlling charge-density-wave states in nano-thick crystals of 1T-TaS2. Sci. Rep., 4, 7302.
115. Tsen, A.W.; Hovden, R.;Wang, D.; Kim, Y.D.; Okamoto, J.; Spoth, K.A.; Liu, Y.; Lu,W.; Sunf, Y.; James, C. (2015). Structure and control of charge density waves in two-dimensional 1T-TaS2. Proceeding National Academic Science, USA, 112, pp: 15054-15059.
116. Song, L.; Ci, L.; Lu, H.; Sorokin, P. B.; Jin, C.; Ni, J.; Kvashnin, A. G.; Kvashnin, D. G.; Lou, J.; Yakobson, B. I.; et al. (2010). Large Scale Growth and Characterization of Atomic Hexagonal Boron Nitride Layers. Nano Letter, 10, pp: 3209-3215.
117. Xi, X.; Zhao, L.; Wang, Z.; Berger, H.; Forro, L.; Shan, J.; Mak, K. F. (2015). Strongly enhanced charge-density-wave order in monolayer NbSe2. Nature Nanotechnology, 10, pp: 765-769.
118. Ugeda, M. M.; Bradley, A. J.; Zhang, Y.; Onishi1, S.; Chen, Y.; Ruan,W.; Aristizaba, C. O.; Ryu, H.; Mark, T.; Edmonds, M. T. (2016). Characterization of collective ground states in single-layer NbSe2. Nat. Phys., 12, pp: 92-97.
119. Schliehe, C.; Juarez, B. H.; Pelletier, M.; Jander, S.; Greshnykh, D.; Nagel, M.; Meyer, A.; Foerster, S.; Kornowski, A.; Klinke, C. (2010). Ultra-thin PbS Sheets by Two-Dimensional Oriented Attachment. Science, 329, pp: 550-553.
120. Bizeto, M. A.; Shiguihara, A. L.; Constantino, V. R. L. (2009). Layered Niobate Nanosheets: Building Blocks for Advanced Materials Assembly. Journal of Material Chemistry, 19, pp: 2512-2525.
121. Ebina, Y.; Sasaki, T.; Watanabe, M. (2002). Study on Exfoliation of Layered Perovskite-

Type Niobates. Solid State Ionics, 151, pp: 177-182.

122. Ding, Z.; Bux, S. K.; King, D. J.; Chang, F. L.; Chen, T.-H.; Huang, S.-C.; Kaner, R. B. (2009). Lithium Intercalation and Exfoliation of Layered Bismuth Selenide and Bismut Telluride. Journal of Material Chemistry, 19, pp: 2588-2592.
123. Fukuda, K.; Akatsuka, K.; Ebina, Y.; Ma, R.; Takada, K.; Nakai, I.; Sasaki, T. (2008). Exfoliated Nano-sheet Crystallite of Cesium Tungstate with 2D Pyrochlore Structure: Synthesis, Characterization, and Photochromic Properties. ACS Nano, 2, pp: 1689-1695.
124. Aksit, M.; Toledo, D. P.; Robinson, R. D. (2012). Scalable Nano-manufacturing of Millimetre-Length 2D NaxCoO2 Nanosheets. Journal of Material Chemistry, 22, pp: 5936-5944.
125. Sheneve Z. Butler, Shawna M. Hollen, Linyou Cao, Yi Cui, Jay A. Gupta, Humberto R. Gutie rrez, Tony F. Heinz, Seung Sae Hong, Jiaxing Huang, Ariel F. Ismach, Ezekiel Johnston-Halperin, Masaru Kuno, Vladimir V. Plashnitsa, Richard D. Robinson, Rodney S. Ruoff, Sayeef Salahuddin, Jie Shan, Li Shi,O Michael G. Spencer, Mauricio Terrones, Wolfgang Windl, and Joshua E. Goldberger (2013). Progress, Challenges, and Opportunities in Two-Dimensional Materials Beyond Graphene, ACS Nano, 7(4), pp: 2898-2926.
126. Li, G. & Andrei, E. Y. (2007). Observation of Landau Levels of Dirac Fermions in Graphite. Nat. Phys., 3, 623-627.
127. Miller, D. L.; Kubista, K. D.; Rutter, G. M.; Ruan, M.; de Heer, W. A.; First, P. N.; Stroscio, J. A. (2009). Observing the Quantization of Zero Mass Carriers in Graphene. Science, 324, pp: 924-927.
128. Helveg, S.; Lauritsen, J. V.; Laegsgaard, E.; Stensgaard, I.; Norskov, J. K.; Clausen, B. S.; Topsoe, H.; Besenbacher, F. (2000). Atomic-Scale Structure of Single-Layer MoS2 Nanoclusters. Phys. Rev. Lett., 84, pp: 951-954.
129. Auwarter, W.; Kreutz, T. J.; Greber, T.; Osterwalder, J. (1999). XPD and STM Investigation of Hexagonal Boron Nitride on Ni(111). Surface Science, 429, pp: 229-236.
130. Brar, V. W.; Decker, R.; Solowan, H. M.; Wang, Y.; Maserati, L.; Chan, K. T.; Lee, H.; Girit, C. O.; Zettl, A.; Louie, S. G. (2011). Gate-Controlled Ionization and Screening of Cobalt Adatoms on a Graphene Surface. Nat. Phys., 7, pp: 43-47.
131. Gyamfi, M.; Eelbo, T.; Wasniowska, M.; Wiesendanger, R. Fe (2011) Adatoms on Graphene/Ru(0001): Adsorption Site and Local Electronic Properties. Phys. Rev., 84, 4.
132. Brihuega, I.; Michaelis, C. H.; Zhang, J.; Bose, S.; Sessi, V.; Honolka, J.; Schneider, M. A.; Enders, A.; Kern, K. (2008). Electronic Decoupling and Templating of CO Nanocluster Arrays on the Boron Nitride Nanomesh. Surface Science, 602, pp: L95-L99.
133. Natterer, F. D.; Patthey, F.; Brune, H. (2012). Ring State for Single Transition Metal Atoms on Boron Nitride on Rh(111). Phys. Rev. Lett., 109, 066101.
134. Besenbacher, F.; Lauritsen, J. V.; Linderoth, T. R.; Laegsgaard, E.; Vang, R. T.; Wendt, S. (2009). Atomic-Scale Surface Science Phenomena Studied by Scanning Tunneling Microscopy. Surface Science, 603, pp: 1315-1327.
135. Krivanek, O. L.; Chisholm, M. F.; Nicolosi, V.; Pennycook, T. J.; Corbin, G. J.; Dellby, N.; Murfitt, M. F.; Own, C. S.; Szilagyi, Z. S.; Oxley, M. P. (2010). Atom-by-Atom Structural and Chemical Analysis by Annular Dark-Field Electron Microscopy. Nature, 464, pp: 571-574.
136. Gutirrez, H. R.; Perea-Lopez, N.; Elias, A. L.; Berkdemir, A.; Wang, B.; Lv, R.; Lopez-Urias, F.; Crespi, V. H.; Terrones, M. (2012). Extra-ordinary Room-Temperature Photoluminescence in WS2 Monolayers. Nano Letter, DOI: 10.1021/nl3026357.
137. Ma, D.; Wang, Q.; Li, T.; Tang, Z.; Yang, G.; He, C.; Lu, Z. (2015). CO catalytic oxidation on Al-doped graphene-like ZnO mono-layer sheets: A first-principles study. Journal of Material Chemistry, 3, pp: 9964-9972.
138. Rao, G. S.; Hussain, T.; Islam, M. S.; Sagynbaeva, M.; Gupta, D.; Panigrahi, P.; Ahuja, R. (2016). Adsorption mechanism of graphene-like ZnO

mono-layer towards CO2 molecules: enhanced CO2 capture. Nanotechnology, 27, 015502.
139. Zhang, Y.H.; Zhang, M.L.; Zhou, Y.C.; Zhao, J.H.; Fanga, S.M.; Li, F. (2014). Tunable electronic and magnetic properties of graphene-like ZnO mono-layer upon doping and CO adsorption: A first-principles study. Journal of Material Chemistry, 2, 13129.
140. Chaojie Cui, Fei Xue, Wei-Jin Hu, Lain-Jong Li (2008). Two-dimensional materials with piezoelectric and ferroelectric Functionalities. Nature Partner Journals, 2D materials and applications. Retrieved from www.nature.com/npj2dmaterials
141. Wu, W. (2014). Piezoelectricity of single-atomic-layer MoS2 for energy conversion and piezotronics. Nature, 514, 470.
142. Lee, J. H. (2017). Reliable piezoelectricity in bilayer WSe2 for piezoelectric nanogenerators. Advanced Materials 29, 1606667.
143. Hao, C. (2016). Flexible all-solid-state supercapacitors based on liquid-exfoliated black-phosphorus nanoflakes. Advanced Materials, 28, pp: 3194-3201.
144. Kulish, V. V., Malyi, O. I., Persson, C. & Wu, P. (2015). Phosphorene as an anode material for Na-ion batteries: a first-principles study. Phys. Chem. Chem. Phys. 17, pp: 13921-13928.
145. A. Castellanos-Gomez, M. Poot, G. A. Steele, H. S. J. Van Der Zant, N. Agrait, G. Rubio-Bollinger, (2012). Elastic properties of freely suspended MoS2 nanosheets, Advanced Materials, 24, pp: 772-775.
146. J. Pu, Y. Yomogida, K. K. Liu, L. J. Li, Y. Iwasa, T. Takenobu (2012). Highly flexible MoS2 thin-film transistors with ion gel dielectrics, Nano Letters 12, pp: 4013-4017.
147. M. Y. Zavodchikova, T. Kulmala, A. G. Nasibulin, V. Ermolov, S. Franssila, K. Grigoras, E. I. Kauppinen (2009). Carbon nanotube thin film transistors based on aerosol methods, Nanotechnology, 20, 085201.
148. D.-M. Sun, M. Y. Timmermans, Y. Tian, A. G. Nasibulin, E. I. Kauppinen, S. Kishimoto, T. Mizutani, Y. Ohno, (2011). Flexible high-performance carbon nanotube integrated circuits, Nature Nanotechnology 6, pp: 156-161.
149. M. S. Arnold, A. S. Green, J. F. Hulvat, S. I. Stupp, M. C. Hersam (2006). Sorting carbon nanotubes by electronic structure using density differentiation, Nature nanotechnology, 1, pp: 60-65.
150. M. Singh, H. M. Haverinen, P. Dhagat, G. E. Jabbour (2010). Inkjet printing-process and its applications, Advanced Materials, 22, pp: 673-685.
151. Z. Yin, H. Li, H. Li, L. Jiang, Y. Shi, Y. Sun, G. Lu, Q. Zhang, X. Chen, H. Zhang (2012). Single-layer MoS2 phototransistors, ACS Nano, 6, pp: 74-80.
152. O. Lopez-Sanchez, D. Lembke, M. Kayci, A. Radenovic, A. Kis, (2013). Ultrasensitive photodetectors based on monolayer MoS2, Nature Nanotechnology, 8, pp: 497-501.
153. A. Abderrahmane, P. J. Ko, T. V. Thu, S. Ishizawa, T. Takamura, A. Sandhu (2014). High photosensitivity few-layered MoSe2 back-gated field-effect phototransistors, Nanotechnology, 25, 365202.
154. N. Huo, S. Yang, Z. Wei, S.-S. Li, J.-B. Xia, J. Li (2014). Photo-responsive and gas sensing field-effect transistors based on multilayer WS2 nanoflakes., Scientific reports, 4, 5209.
155. W. Zhang, M. H. Chiu, C. H. Chen, W. Chen, L. J. Li, A. T. S. Wee (2014). Role of metal contacts in high-performance phototransistors based on WSe2 monolayers, ACS Nano, 8, pp: 8653-8661.
156. X. Hong, J. Kim, S.-F. Shi, Y. Zhang, C. Jin, Y. Sun, S. Tongay, J.Wu, Y. Zhang, F. Wang (2014). Ultrafast charge transfer in atomically thin MoS2/WS2 heterostructures, Nature Nanotechnology, 9, pp: 1-5.
157. F. H. Koppens, T Mueller, P Avouris, A. C. Ferrari, M. S. Vitiello, M Polini (2014). Photodetectors based on graphene, other two-dimensional materials and hybrid systems, Nature Nanotechnology, 9, pp: 780-793.
158. Li F, Zhao S-F, Chen L, Khan A, MacFarlane D. R., Zhang J. (2016). Polyethylenimine promoted electrocatalytic reduction of CO2 to CO in aqueous medium by graphene-supported amorphous molybdenum sulphide. Energy and Environmental Science; 9, pp: 216-223.

159. Chan K., Tsai C., Hansen H. A., Norskov J. K. (2014). Molybdenum sulfides and selenides as possible electrocatalysts for CO2 reduction. Chemical Catalyst Chemistry; 6, pp: 1899-1905.
160. Shi C., Hansen H. A., Lausche A. C., Norskov J.K. (2014). Trends in electrochemical CO2 reduction activity for open and close-packed metal surfaces. Physical Chemistry Chemical Physics; 16, pp: 4720-4727.
161. Asadi M., Kumar B., Behranginia A., Rosen B. A., Baskin A., Repnin N. (2014). Robust carbon dioxide reduction on
162. molybdenum disulphide edges. Nature Communications; 5: 4470